Definition of the Structural Elements in Plasminogen Required for High-Affinity Binding to Apolipoprotein(a): A Study Utilizing Surface Plasmon Resonance†

Mark A. Hancock, Craig A. Spencer, and Marlys L. Koschinsky*

Department of Biochemistry, Queen's University, Kingston, Ontario, Canada K7L 3N6

Received June 15, 2004; Revised Manuscript Received July 19, 2004

ABSTRACT: Lipoprotein(a) [Lp(a)] is suggested to link atherosclerosis and thrombosis owing to the similarity between the apolipoprotein(a) [apo(a)] moiety of Lp(a) and plasminogen. Lp(a) may interfere with tPA-mediated plasminogen activation in fibrinolysis, thereby generating a hypercoaguable state in vivo. The present study employed surface plasmon resonance (SPR) to examine the binding interaction between plasminogen and a physiologically relevant, 17-kringle recombinant apo(a) species [17K r-apo(a)] in real time. Native, intact Glu[1]-plasminogen bound to apo(a) with substantially higher affinity ($K_D \sim 0.3$ μM) compared to a series of plasminogen fragments (K1−5, K1−3, K4, K5P, and tail domain) that interacted weakly with apo(a) ($K_D > 50$ μM). Treatment of Glu[1]-plasminogen with citraconic anhydride (a lysine modification reagent) completely abolished binding to wild-type 17K r-apo(a), whereas citraconylated 17K r-apo(a) decreased binding to wild-type Glu[1]-plasminogen by ∼50%; inhibition of binding was also observed using the lysine analogue ϵ-aminocaproic acid. Whereas native Glu[1]-plasminogen exhibited monophasic binding to 17K r-apo(a), truncated Lys[78]-plasminogen exhibited biphasic binding. Altering Glu[1]-plasminogen from its native, closed conformation (in chloride buffer) to an open conformation (in acetate buffer) also yielded biphasic isotherms. These SPR data are consistent with a two-state kinetic model in which a conformational change in the plasminogen−apo(a) complex may occur following the initial binding event. Differential binding kinetics between Glu[1]-/Lys[78]-plasminogen and apo(a) may explain why Lp(a) is a stronger inhibitor of tPA-mediated Glu[1]-plasminogen activation compared to Lys[78]-plasminogen activation.

Elevated plasma levels of lipoprotein(a) [Lp(a)[1]] have been identified as a risk factor for the development of atherosclerotic disorders including coronary heart disease (reviewed in ref *1*). Originally described by Berg (*2*), Lp(a) is similar to low-density lipoprotein (LDL) in that it contains a cholesteryl ester core surrounded by a monolayer of unesterified cholesterol and phospholipid in which apolipoprotein B-100 (apoB-100) is embedded. Lp(a) is distinct from LDL in that it contains a single molecule of an additional glycoprotein moiety called apolipoprotein(a) [apo(a)], which is covalently linked to apoB-100 by a single disulfide bond (*3*, *4*). The cloning of apo(a) (*5*) revealed a striking similarity between the sequence of apo(a) and the fibrinolytic serine protease zymogen plasminogen.

The native form of plasminogen (Glu[1]-plasminogen) contains an N-terminal tail domain of 77 amino acids, five intervening kringle domains (K1−K5), and a trypsin-like protease domain at the C terminus (*6*, *7*). Binding studies with lysine and its analogues have shown that the K1, K4, and K5 domains contain strong, moderate, and weak affinity lysine-binding sites (LBS), respectively, whereas K2 contains a very weak LBS and K3 does not contain a functional LBS (*8*−*10*). In solution, Glu[1]-plasminogen exists in a closed-loop, activation-resistant conformation that is stabilized by interactions between lysine residues in the tail domain and sequences in the K4 and/or K5 domain (*11*, *12*). Modulators of Glu[1]-plasminogen conformation include chloride ions, acetate ions, lysine analogues such as ϵ-aminocaproic acid (ϵ-ACA), and lysine residues exposed on biological substrates such as fibrin (*13*−*16*). Proteolysis of the Lys[77]−Lys[78] peptide bond (plasminogen amino acid numbering system includes Gln residue at sequence position 32; see ref *44*) by plasmin results in the generation of a truncated form of plasminogen denoted Lys[78]-plasminogen (*17*, *18*). Loss of

† This work was supported by Heart and Stroke Foundation of Ontario Grant-In-Aid T-4408 (to M.L.K.). M.L.K. is a Career Investigator of the Heart and Stroke Foundation of Ontario. Financial support for the BIACORE 3000 instrumentation was provided through the Canadian Foundation for Innovation and the Queen's University Protein Function Discovery Program.

* Author to whom correspondence should be addressed [telephone (613) 533-6586; fax (613) 533-2987; e-mail mk11@post.queensu.ca].

[1] Abbreviations: 17K, 17-kringle; ϵ-ACA, ϵ-aminocaproic acid; apo(a), apolipoprotein(a); apoB-100, apolipoprotein B-100; BHK, baby hamster kidney (cells); BSA, bovine serum albumin; *C*, concentration of analyte in solution; CM5, carboxymethylated dextran matrix sensor chip; DFP, diisopropylfluorophosphate; DTT, dithiothreitol; ELISA, enzyme-linked immunosorbent assay; FDP, degraded fibin cofactors; Flu, fluorescein-labeled; HBS, HEPES-buffered saline; k_a, association rate constant; k_d, dissociation rate constant; K_D, equilibrium dissociation constant; K, kringle; LBS, lysine-binding site; LDL, low-density lipoprotein; Lp(a), lipoprotein(a); MTL, mass transport limitation; P20, Biacore surfactant; PBS, phosphate-buffered saline; PEG, poly(ethylene glycol); Pg, plasminogen (amino acid numbering system includes Gln residue at sequence position 32; see ref *44*); PPE, porcine pancreatic elastase; r-apo(a), recombinant apo(a); R_{eq}, steady-state binding level; RIA, radiolabeled immunosorbant assay; R_{max}, maximum analyte binding capacity; RU, resonance unit(s); SDS−PAGE, sodium dodecyl sulfate−polyacrylamide gel electrophoresis; SPR, surface plasmon resonance; tPA, tissue-type plasminogen activator; VFK-CK, D-Val-Phe-Lys-chloromethyl ketone dihydrochloride.

10.1021/bi048756o CCC: $27.50
Published on Web 08/28/2004

the tail domain also induces a large conformational change such that Lys^{78}-plasminogen is characterized by a flexible open-loop structure in which the activation cleavage site ($Arg^{561}-Val^{562}$) is exposed (*19*−*21*). During fibrinolysis, the increased affinity of Lys^{78}-plasminogen for fibrin cofactor and tissue-type plasminogen activator (tPA) renders it a more efficient substrate for plasminogen activation compared to Glu^1-plasminogen (*22*, *23*).

The apo(a) moiety of Lp(a) lacks sequences corresponding to the plasminogen tail and kringle 1, 2, and 3 domains, yet contains multiple repeats of plasminogen K4-like domains [apo(a) KIV] followed by plasminogen K5-like [apo(a) KV] and protease-like domains (*5*). There are 10 distinct classes of apo(a) KIV repeats (designated KIV_1-KIV_{10} domains), which differ from one another by only a small number of amino acid substitutions (*5*). There is a single copy of each KIV repeat except for KIV_2, which is known as the major repeat kringle (*24*, *25*). This sequence can be present in 3−>30 identical copies, which gives rise to Lp(a) isoform size heterogeneity in the population (*26*). Apo(a) KIV_{5-8} each contain a weak lysine-binding site (LBS) that mediates the initial non-covalent interaction between apo(a) and apoB-100 in the assembly of Lp(a) (*27*−*29*). Apo(a) KIV_9 contains an unpaired cysteine residue that forms the disulfide linkage with apoB-100 in the Lp(a) assembly (*3*, *4*). Apo(a) KIV_{10} contains a stronger LBS that is believed to mediate binding of apo(a)/Lp(a) to lysine residues exposed on biological substrates such as fibrin (*30*, *31*). Due to the presence of a critical amino acid substitution and a deletion of several amino acid residues, the apo(a) protease-like domain exhibits no catalytic activity (*32*).

The similarity of Lp(a) to both LDL and plasminogen suggests that the pathogenic mechanism of Lp(a) likely involves both proatherogenic and prothrombotic/antifibrinolytic effects (reviewed in ref *1*). Several in vitro and in vivo studies have shown that apo(a) or intact Lp(a) can inhibit fibrinolysis (*33*−*35*). Moreover, binding interactions have been demonstrated between apo(a)/Lp(a) and fibrin(ogen), plasmin-modified fibrin(ogen), plasminogen, and tPA (*30*, *36*−*40*). We have recently proposed that the inhibition of plasminogen activation by Lp(a) conforms to an equilibrium template model in which apo(a) can interact with all three ternary complex members (tPA, plasminogen, fibrin), as opposed to a direct competition between apo(a) and plasminogen for binding sites on fibrin (*41*). Our previous studies have demonstrated a high-affinity interaction between apo(a)/Lp(a) and plasminogen (*38*), so the present study sought to provide a more detailed analysis of the structural elements in plasminogen that mediate this binding interaction. Using surface plasmon resonance (SPR) and a series of native plasminogen fragments, we demonstrate that native, intact Glu^1-plasminogen is required for maximal binding to apo(a) and that Lys^{78}-plasminogen exhibits distinctly different binding kinetics for apo(a) compared to Glu^1-plasminogen. In additional kinetic studies using a fluorescently labeled, catalytically inactive form of plasminogen, we demonstrate that apo(a) is a strong inhibitor of tPA-mediated Glu^1-plasminogen activation but a relatively poor inhibitor of Lys^{78}-plasminogen activation.

MATERIALS AND METHODS

Materials. Benzamidine−Sepharose (affinity), lysine−Sepharose CL-4B (affinity), and Q-Sepharose (ion-exchange) resins were from Amersham Biosciences (Baie d'Urfe, PQ, Canada). Bio-Gel P-60 (gel filtration) resin was from Bio-Rad (Hercules, CA). All SPR instrumentation, software, and reagents (including P20 surfactant) were from Biacore Inc. (Piscataway, NJ). The plasmin-specific inhibitor D-Val-Phe-Lys chloromethyl ketone (VFK-CK) was from Calbiochem (San Diego, CA). The plasmin-specific chromogenic substrate S-2251 was from Chromogenix AB (Molndal, Sweden). Dialysis tubing (3.5 kDa MWCO) and dithiothreitol (DTT) were from Fisher Scientific Limited (Nepean, ON, Canada). Poly(ethylene glycol) (PEG) 20000 was from Fluka (Seelze, Germany). Mammalian cell culture media, sera, and reagents were from Gibco Invitrogen Corp. (Burlington, ON, Canada). Citraconic anhydride was from ICN Biomedicals Inc. (Costa Mesa, CA). Units of citrated, fresh frozen, human plasma were from Kingston General Hospital (Kingston, ON, Canada). Centricons (4 mL; 30 kDa NMWL) were from Millipore Corp. (Bedford, MA). Porcine pancreatic elastase (PPE) was from Roche Diagnostics (Laval, PQ, Canada). ϵ-Aminocaproic acid (ϵ-ACA) and diisopropylfluorophosphate (DFP) were from Sigma-Aldrich Canada Limited (Oakville, ON, Canada). Purified human plasmin and thrombin were generously provided by Dr. Michael E. Nesheim (Queen's University) and were prepared from plasma-derived plasminogen and prothrombin, respectively, as previously described (*42*). All materials required for the fluorescent plasminogen activation assays were prepared as previously described (*41*).

Expression and Purification of Recombinant Apo(a). Construction of the 17-kringle recombinant apo(a) variant in the pRK5 expression plasmid (pRK5ha17) has been previously described (*43*). Baby hamster kidney (BHK) cells were cultured in 100 mm dishes using DMEM/F12 medium supplemented with 5% newborn calf serum. For stable 17K r-apo(a) expression, BHK cells were cotransfected with the pRK5ha17 and neomycin resistance plasmids using calcium phosphate precipitation; neomycin-resistant foci were isolated using the selective agent G418, and positive clones were identified by ELISA/Western blotting as previously described (*43*). Subsequently cultured in conditioned medium (Opti-MEM), the 17K r-apo(a) protein secreted from the BHK cells was purified by affinity chromatography as previously described (*29*). Briefly, Opti-MEM harvests collected from the stably transfected cells were loaded over a 50 mL lysine−Sepharose column pre-equilibrated in PBS (2.7 mM KCl, 1.8 mM KH_2PO_4, 137 mM NaCl, 10.1 mM Na_2HPO_4, pH 7.4). The column was washed extensively with PBS containing 500 mM NaCl, and r-apo(a) was eluted with 200 mM ϵ-ACA in the same buffer. Protein-containing fractions were pooled, dialyzed extensively against HBS (20 mM HEPES, 150 mM NaCl, pH 7.4), and concentrated using PEG 20000. Aliquots of purified protein were stored at −70 °C prior to use. All protein concentrations were determined spectrophotometrically (corrected for Rayleigh scattering) using the following molecular weight and extinction coefficient: 17K [MW ∼ 278 719; $\epsilon_{1\%}(280\ nm) = 20.7$]. The 17K r-apo(a) proteins were assessed for purity by SDS−PAGE (0.5 μg/lane; 4−20% polyacrylamide gradient) under nonreducing

and reducing (containing 10 mM DTT) conditions followed by silver staining. All purified 17K r-apo(a) preparations appeared as homogeneous bands under both nonreducing and reducing conditions and migrated at the expected molecular weight.

Purification of Native Plasminogen. Glu[1]-plasminogen (Glu[1]−Asn[791]) was purified from citrated, fresh frozen, human plasma by lysine−Sepharose affinity chromatography as previously described (*44*) with several modifications. Briefly, 1 L of plasma was passed over 160 mL of lysine−Sepharose resin (pre-equilibrated in 0.1 M sodium phosphate buffer, pH 8.0) in a 350 mL sintered glass funnel under low vacuum. The resin was then stacked in a column (2.5 × 30 cm) and washed at 4 °C with 0.1 M sodium phosphate buffer, pH 8.0, overnight. Specifically bound plasminogen was eluted from the column in wash buffer containing 20 mM ϵ-ACA. To remove contaminating serine protease activity, protein-containing fractions were pooled and then passed over a 4 mL benzamidine−Sepharose column pre-equilibrated in wash buffer. Pre- and post-chromatography aliquots were monitored for a lack of hydrolysis of the plasmin-specific chromogenic substrate S-2251 at 405 nm in a Lambda-4B spectrophotometer (Perkin-Elmer, Boston, MA) in kinetics mode. The plasmin-free flow-through was concentrated at 4 °C by adding ammonium sulfate (80% saturation), stirring overnight, and centrifugation at 10000*g* for 20 min. The pellet was resuspended in a minimal volume of HBS and then centrifuged at 3000*g* for 5 min at 22 °C; the supernatant was extracted and saved for dialysis. The pellet was washed two more times in a minimal volume of HBS, extracting and saving the supernatant each time. The supernatant volumes were pooled and dialyzed against HBS at 4 °C. Aliquots of purified protein were stored at −70 °C prior to use. All protein concentrations were determined spectrophotometrically (corrected for Rayleigh scattering) using the following molecular weight and extinction coefficient: Glu[1]-plasminogen [MW ∼ 92 000; $\epsilon_{1\%}$(280 nm) = 16.1]. The Glu[1]-plasminogen proteins were assessed for purity by SDS−PAGE (0.5 μg/lane; 4−20% polyacrylamide gradient) under nonreducing and reducing (containing 10 mM DTT) conditions followed by silver staining. All purified Glu[1]-plasminogen preparations appeared as homogeneous bands under both nonreducing and reducing conditions and migrated at the expected molecular weight.

Citraconic Anhydride Modification. 17K r-apo(a) and Glu[1]-plasminogen were modified with citraconic anhydride as previously described (*45*) with several modifications. Briefly, each protein stock (2 mg/mL) was added to a saturated sodium acetate solution (15 g in 35 mL of dH_2O) in a 1:1 ratio. After incubation on a shaker for 15 min at 4 °C, citraconic anhydride (145 μM final) was added in 2 μL increments every 15 min. The treated sample volumes were then dialyzed extensively against HBS at 4 °C. Aliquots of purified protein were stored at −70 °C prior to use. All citraconic anhydride-modified protein concentrations were determined spectrophotometrically (corrected for Rayleigh scattering) using the molecular weights and extinction coefficients specified above. Control proteins (positively charged, native lysine residues) and modified proteins (negatively charged, derivatized lysine residues) appeared as homogeneous bands as assessed by native agarose electrophoresis [5 μg/lane; 1% agarose for 17K r-apo(a); 2% agarose for Glu[1]-plasminogen] with Coomassie Blue staining. The citraconic anhydride treatment was reversible upon incubation of the modified proteins in HBS under low-pH (5.0) conditions, followed by incubation in HBS under physiological pH (7.4) conditions.

Purification of Native Plasminogen Fragments. The plasminogen tail domain (Glu[1]−Lys[77]) and Lys[78]-plasminogen (Lys[78]−Asn[791]) were isolated following plasmin-mediated digestion of Glu[1]-plasminogen as previously described (*46*) with several modifications. Briefly, Glu[1]-plasminogen (10 mg/mL), ϵ-ACA (5 mM), and plasmin (0.25 μM) were incubated in 2 mL of HBS (final volume). After 90 min at 22 °C, the reaction mixture was passed over a 1 mL aprotinin−agarose column pre-equilibrated in HBS. Pre- and post-chromatography aliquots were monitored for a lack of hydrolysis of the plasmin-specific chromogenic substrate S-2251 as specified above. The plasmin-free flow-through was also treated with VFK-CK (10 μM final) for 1 h at 4 °C. The sample volume was then diluted 1/5 in HBS prior to passage over a 30 mL lysine−Sepharose column pre-equilibrated in HBS.

Protein-containing, lysine−Sepharose wash fractions (plasminogen tail domain in HBS) were pooled and then centrifuged at 22 °C at 3000*g* in 4 mL centricons with 30 kDa molecular weight cutoff filters. The plasminogen tail domain was collected in the flow-through, whereas traces of Lys[78]-plasminogen were retained above the filter. The flow-through volumes were pooled and diluted 1/5 in 20 mM HEPES, pH 7.4, prior to passage over a 1 mL Q-Sepharose column pre-equilibrated in the same buffer. After washing, the plasminogen tail domain was eluted with HBS containing 0.5 M NaCl and then dialyzed against HBS at 4 °C. Aliquots of purified protein were stored at −70 °C prior to use. All protein concentrations were determined spectrophotometrically (corrected for Rayleigh scattering) using the following molecular weight and extinction coefficient: plasminogen tail domain [MW ∼ 8794; $\epsilon_{1\%}$(280 nm) = 3.0]. The plasminogen tail domain proteins were assessed for purity by SDS−PAGE (0.5 μg/lane; 4−20% polyacrylamide gradient) under nonreducing and reducing (containing 10 mM DTT) conditions followed by silver staining. All purified plasminogen tail domain preparations appeared as homogeneous bands under both nonreducing and reducing conditions and migrated at the expected molecular weight.

Protein-containing, lysine−Sepharose elution fractions (Lys[78]-plasminogen in HBS containing 20 mM ϵ-ACA) were pooled and concentrated at 4 °C by adding ammonium sulfate (80% saturation), stirring overnight, and centrifugation at 10000*g* for 20 min. The pellet was resuspended in a minimal volume of HBS and then centrifuged at 3000*g* for 5 min at 22 °C; the supernatant was extracted and saved for dialysis. The pellet was washed two more times in a minimal volume of HBS, extracting and saving the supernatant each time. The supernatant volumes were pooled and then dialyzed against HBS at 4 °C. Aliquots of purified protein were stored at −70 °C prior to use. All protein concentrations were determined spectrophotometrically (corrected for Rayleigh scattering) using the following molecular weight and extinction coefficient: Lys[78]-plasminogen [MW ∼ 84 000; $\epsilon_{1\%}$-(280 nm) = 16.1]. The Lys[78]-plasminogen proteins were assessed for purity by SDS−PAGE (0.5 μg/lane; 7%

polyacrylamide) under nonreducing and reducing (containing 10 mM DTT) conditions followed by silver staining. All purified Lys^{78}-plasminogen preparations appeared as homogeneous bands under both nonreducing and reducing conditions and migrated at the expected molecular weight.

Elastase-derived plasminogen fragments (PgK1−3, Tyr^{80}−Val^{345}; PgK4, Val^{355}−Ala^{440}; PgK5P, Leu^{450}−Asn^{791}) were isolated as previously described (*47*) with several modifications. Briefly, 160 mg of Glu^1-plasminogen and 720 μg of porcine pancreatic elastase (PPE) were diluted in 13 mL (final volume) of reaction buffer (0.3 M NH_4HCO_3, pH 8.3). After 5 h at 22 °C, the reaction was terminated by passage over a 4 mL benzamidine−Sepharose column, pre-equilibrated in the same buffer. The PPE-free flow-through was also treated with DFP (to 2 mM) and incubated for 30 min at 4 °C. The reaction mixture was then adjusted to 0.55 M with respect to NH_4HCO_3 and stirred overnight at 4 °C prior to passage over a 100 mL lysine−Sepharose column (2.5 × 15 cm) pre-equilibrated in wash buffer (0.1 M NH_4HCO_3, pH 8.3). The column was washed with the same buffer; the fragment containing the plasminogen kringle 5 and protease domains (PgK5P) was present in the wash fractions. To ensure that the PgK5P fractions were catalytically inactive, they were monitored for a lack of hydrolysis of the plasmin-specific chromogenic substrate S-2251 as specified above. Specifically bound fragments corresponding to plasminogen kringles 1−3 (PgK1−3) and kringle 4 (PgK4) were eluted from the column with wash buffer containing 20 mM ϵ-ACA. Protein-containing wash and elution fractions were appropriately pooled in dialysis tubing and concentrated using PEG 20000. Subsequent passages over 350 mL Bio-Gel P-60 columns (1.5 × 160 cm; 23 mL/min flow rate; 2.5 mL fractions) in wash buffer resulted in the separation of catalytically inactive PgK5P [MW ∼ 38 000; ϵ(280 nm) = 8.9×10^4 M^{-1} cm^{-1}] from any residual, DFP-bound PPE (MW ∼ 26 000), and the separation of PgK1−3 [MW ∼ 38 000; ϵ(280 nm) = 8.0×10^4 M^{-1} cm^{-1}] from PgK4 [MW ∼ 11 000; ϵ(280 nm) = 3.1×10^4 M^{-1} cm^{-1}]. Protein-containing fractions corresponding to each fragment were pooled and dialyzed against HBS at 4 °C. Aliquots of purified protein were stored at −70 °C prior to use. All protein concentrations were determined spectrophotometrically (corrected for Rayleigh scattering) using the molecular weights and extinction coefficients specified above. The elastase-derived proteins were assessed for purity by SDS−PAGE (0.5 μg/lane; 4−20% polyacrylamide gradient) under nonreducing and reducing (containing 10 mM DTT) conditions followed by silver staining. All purified fragment preparations appeared as homogeneous bands under both nonreducing and reducing conditions and migrated at the expected molecular weights.

Additionally, a plasmin-derived plasminogen fragment (PgK1−5, Lys^{78}−Arg^{530}) was isolated as previously described (*48*) with several modifications. Briefly, 4 mg of plasmin was dialyzed against 0.1 M glycine−NaOH, pH 10.5, at 4 °C and then added to 40 mg of Glu^1-plasminogen in 10 mL of the same buffer (final volume). After 12 h at 37 °C, the reaction mixture was dialyzed against 0.1 M sodium phosphate, pH 8.0, at 4 °C overnight before passage over a 4 mL benzamidine−Sepharose column pre-equilibrated in the same buffer. Pre- and post-chromatography aliquots were monitored for a lack of hydrolysis of the plasmin-specific chromogenic substrate S-2251 as specified above. The plasmin-free flow-through was then passed over a 10 mL lysine−Sepharose column pre-equilibrated in the sodium phosphate buffer. The column was washed with the same buffer, and the specifically bound PgK1−5 fragment [MW ∼ 55 000; $\epsilon_{1\%}$(280 nm) = 17.0] was eluted with sodium phosphate buffer containing 20 mM ϵ-ACA. Protein-containing fractions were pooled and dialyzed against HBS at 4 °C. Aliquots of purified protein were stored at −70 °C prior to use. All protein concentrations were determined spectrophotometrically (corrected for Rayleigh scattering) using the molecular weight and extinction coefficient specified above. The PgK1−5 fragments were assessed for purity by SDS−PAGE (0.5 μg/lane; 4−20% polyacrylamide gradient) under nonreducing and reducing (containing 10 mM DTT) conditions followed by silver staining. All purified PgK1−5 preparations appeared as homogeneous bands under both nonreducing and reducing conditions and migrated at the expected molecular weight.

Surface Plasmon Resonance (SPR). The binding interaction between plasminogen *analyte* and apo(a) *ligand* was examined in real time using a BIACORE 3000 biosensor system (Biacore Inc., Piscataway, NJ). Changes in the refractive index at the sensor chip surface over time (caused by analyte−ligand association and dissociation) are scaled in resonance units (RU) (*49*). For proteins, every 1000 RU corresponds to a surface mass change of ∼1 ng/mm^2. All experiments were performed at 25 °C using research grade carboxymethylated dextran matrix (CM5) sensor chips (Biacore Inc.). On-line subtraction (response over active surface less response over reference surface) corrected for bulk refractive index changes, nonspecific binding, and instrument drift. Prior to all analyses, the plasminogen and/or fragment analyte preparations were dialyzed against the running buffer to minimize bulk effects. Blank analyte injections (i.e., running buffer only) were also subtracted from the specific binding isotherms to further minimize instrument noise.

For affinity binding experiments, active flow cells of ∼2000 RU 17K r-apo(a) (50 μg/mL in 10 mM sodium acetate, pH 4.5) were immobilized using the ligand thiol-coupling kit (Biacore Inc.) and running buffer 1 [10 mM HEPES, 150 mM NaCl, 3.4 mM EDTA, 0.005% (v/v) P20 surfactant, pH 7.4]. For kinetic binding experiments, active flow cells of ∼500 RU 17K r-apo(a) (wild-type and citraconic anhydride-modified) were immobilized in a similar manner. For reference flow cells, the surfaces were activated and blocked in a similar manner but in the absence of any ligand addition. In all cases, analyte binding measurements were performed using running buffer 2 [identical to running buffer 1, but containing 0.003% (v/v) P20 surfactant]. Surfaces were regenerated after each binding interaction using running buffer 1 containing 20 mM ϵ-ACA/0.5 M NaCl. Typical parameters for each cycle of the affinity and kinetic binding methods were as follows: 250 μL of analyte (with 750 s of dissociation) at 20 μL/min, 3 × 80 μL regeneration at 40 μL/min, 250 μL of running buffer at 20 μL/min. Association, k_a (M^{-1} s^{-1}), and dissociation, k_d (s^{-1}), rate constants were determined using curve-fitting procedures and binding models available in the BIAevaluation 3.1 software (Biacore Inc.). The association and dissociation phases were fit simultaneously, and global fits were obtained for the k_a and k_d constants. The overall equilibrium dissocia-

tion, K_D (M), constants were obtained from the ratio of the off and on rates ($K_D = k_d/k_a$).

For equilibrium binding experiments, active flow cells of ~1700 RU 17K r-apo(a) were immobilized as specified above. Method parameters for each cycle of the equilibrium binding experiments were as follows: 10 μL of analyte (with 30 s of dissociation) at 40 μL/min, 2 × 10 μL regeneration at 40 μL/min, 2 × 10 μL running buffer at 40 μL/min. To determine the overall equilibrium dissociation constants, binding responses in the steady-state region of the sensorgrams (R_{eq}) were plotted against analyte concentration (C). In the BIAevaluation 3.1 software, the data were subjected to nonlinear regression according to the following equation: $R_{eq} = (C)(R_{max})/(C + K_D)$, where R_{eq} is the steady-state binding level, C is the concentration of analyte in solution, R_{max} is the maximum analyte binding capacity, and K_D is the equilibrium dissociation constant. Alternatively, Scatchard plots were generated (R_{eq}/C vs R_{eq}) and the data were subjected to linear regression according to the following equation: $R_{eq}/C = -(R_{eq}/K_D) + (R_{max}/K_D)$.

Fluorescence Spectroscopy. Intrinsic fluorescence was used to monitor the binding of ϵ-ACA to 17K r-apo(a) and Glu[1]-plasminogen as previously described (*46*, *50*) with several modifications. Briefly, 17K r-apo(a) and Glu[1]-plasminogen were each dialyzed against Biacore buffers A [10 mM HEPES, 150 mM NaCl, 3.4 mM EDTA, 0.003% (v/v) P20 surfactant, pH 7.4] and B [10 mM HEPES, 150 mM sodium acetate, 3.4 mM EDTA, 0.003% (v/v) P20 surfactant, pH 7.4]. In an LS50B fluorescence spectrometer (Perkin-Elmer) thermostated at 22 °C, the four different samples were placed in 4 mL quartz cuvettes with microstir bars [70 nM 17K r-apo(a) or 150 nM Glu[1]-plasminogen], and small aliquots of ϵ-ACA were added [0−100 mM for apo(a) titrations or 0−20 mM for plasminogen titrations]. The additions also contained 17K r-apo(a) or Glu[1]-plasminogen at a concentration identical to that present in the cuvette in order to eliminate the need to correct for dilution. All samples and concentrated ϵ-ACA stocks were diluted in the appropriate chloride- or acetate-containing buffers (A and B, respectively) in each case. Changes in fluorescence intensity were monitored continuously during the course of the titrations [excitation wavelength, 280 nm (slit width = 5.0 nm); emission wavelength, 340 nm (slit width = 5.0 nm); cutoff filter, 290 nm].

Fluorescent Plasminogen Activation Assay. As previously described (*41*), a fluorescence-based system was employed to study the effect of apo(a) on plasminogen activation in the presence of degraded fibrin cofactors (FDP) and in the absence of positive feedback reactions catalyzed by plasmin. Briefly, a recombinant variant of human Glu[1]-plasminogen, in which the active site serine had been replaced by cysteine, was employed so that the zymogen could be labeled with a thiol-specific fluorescein tag (*46*). The labeled protein (Flu-Glu[1]-plasminogen) was digested with plasmin as specified above to generate the fluorescently labeled, truncated form (Flu-Lys[78]-plasminogen). Plasminogen cleavage by tPA was followed at 25 °C using 96-well Dynex Microfluor2 plates and a SpectraMax Gemini XS plate reader (excitation wavelength, 495 nm; emission wavelength, 535 nm; cutoff filter, 530 nm; sensitivity setting, normal; PMT setting, low; run time, 1 h; interval, 36 s). Specifically, 80 μL volumes containing Flu-Glu[1]- or Flu-Lys[78]-plasminogen (0.3 μM final), FDP (0.6 μM final), and 17K r-apo(a) (0−3 μM final) in HBS containing 0.02% (v/v) Tween 80 (HBST) were added to wells already containing 20 μL volumes of tPA (3 nM final) in HBST. Initial rates of fluorescence decrease were compared between the Flu-Glu[1]- and Flu-Lys[78]-plasminogen data sets in the presence of increasing apo(a) concentration.

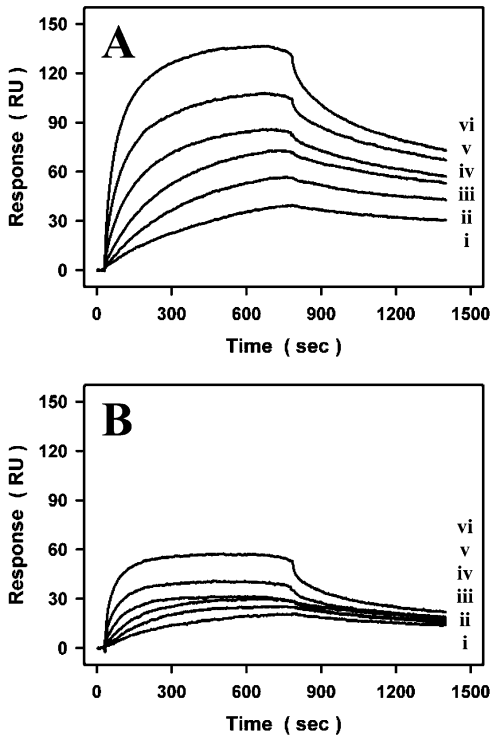

FIGURE 1: SPR analysis of Glu[1]-plasminogen analyte binding to apo(a) ligand at 20 μL/min: representative sensorgrams for specific binding of (i) 0.5, (ii) 1, (iii) 2, (iv) 5, (v) 10, and (vi) 20 μM Glu[1]-plasminogen to wild-type (A) or citraconic anhydride-modified (B) ligand. In each panel, 500 RU of 17K r-apo(a) was immobilized.

RESULTS

The binding interaction between plasminogen and thiol-coupled apo(a) was examined by SPR. The sensorgrams (RU vs time) presented are typical of results acquired in at least three independent trials. The active 17K r-apo(a) surfaces showed good stability, and no significant decreases in bound plasminogen analyte were observed throughout the duration of the experiments. Agreement between the theoretically predicted and experimentally observed maximal specific binding (R_{max}) parameter indicated that the ligand thiol immobilization technique yielded fully active surfaces. Agreement between the theoretical and observed R_{max} values also indicated a 1:1 binding stoichiometry between plasminogen and apo(a). Glu[1]-plasminogen and its fragments exhibited almost no nonspecific binding over reference surfaces [lacking apo(a)] compared to the total responses over apo(a)-immobilized surfaces (data not shown). When BSA (15 μM) or 17K r-apo(a) (5 μM) was injected as the analyte, they also exhibited no nonspecific binding to the reference surfaces (data not shown).

Dose−response experiments with Glu[1]-plasminogen were performed over wild-type and citraconic anhydride-modified 17K r-apo(a) surfaces immobilized in tandem (Figure 1). The titrations showed that Glu[1]-plasminogen binding was sig-

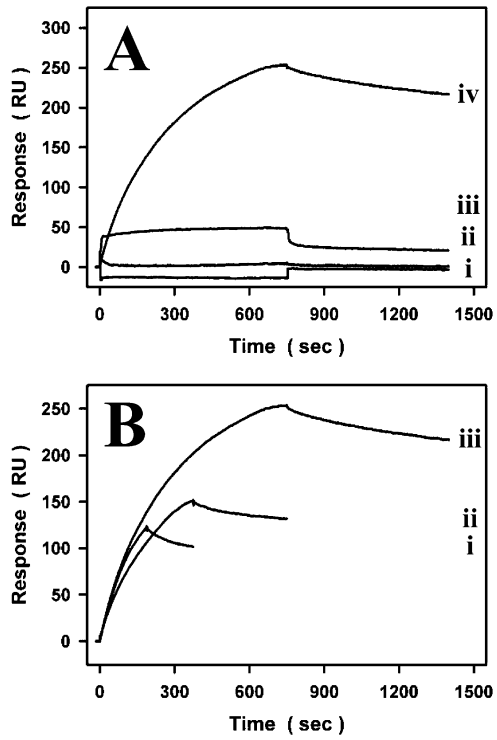

FIGURE 2: SPR analysis of Glu[1]-plasminogen analyte binding to apo(a) ligand at 20 μL/min: (A) representative sensorgrams for specific binding of (i) 1 μM Glu[1]-plasminogen to 17K r-apo(a) with 20 mM ϵ-ACA competitor, (ii) 1 μM citraconic anhydride-modified Glu[1]-plasminogen to 17K r-apo(a), (iii) 1 μM Glu[1]-plasminogen to 17K r-apo(a) with 2 μM 17K r-apo(a) competitor, and (iv) 1 μM Glu[1]-plasminogen to 17K r-apo(a); (B) representative sensorgrams for contact time test in which 1 μM Glu[1]-plasminogen was injected for (i) 188 s, (ii) 375 s, and (iii) 750 s. In each panel, 1700 RU of 17K r-apo(a) was immobilized.

nificantly decreased when citraconic anhydride-modified 17K r-apo(a) was immobilized as the ligand. The binding of Glu[1]-plasminogen to wild-type 17K r-apo(a) was unaltered in the presence of BSA (15 μM) or high 0.5 M salt conditions (data not shown), but significantly decreased in the presence of 17K r-apo(a) as a solution-phase competitor (Figure 2A). Binding was also abolished in the presence of the competitive lysine analogue ϵ-ACA (20−200 mM) or when Glu[1]-plasminogen was pretreated with the lysine modification reagent citraconic anhydride. Thus, the plasminogen-apo(a) binding interaction was very specific as assessed by SPR.

In the BIAevaluation software, initial modeling attempts with the simplest "1:1 (Langmuir) binding" equation failed to provide a good fit to the experimental data as judged by the nonrandom distribution in the residuals. Although mass transport limitation (MTL) effects were not expected with such slow association rates, flow rate tests with low-density immobilized surfaces definitively ruled out the possibility that MTL effects were responsible for the observed deviations from the 1:1 modeling (data not shown). Eventually, it was determined that a more complex "two-state reaction" model provided a good fit to the experimental data. As this model suggests that a conformational change would be occurring in the plasminogen−apo(a) complex after the initial binding event, a contact time test was then performed to assess the validity of the two-state kinetic model (Figure 2B). At a constant flow rate, a fixed concentration of Glu[1]-plasminogen was injected over the wild-type 17K r-apo(a) surface for three different durations. The shortest injection series (188 s) possessed the fastest dissociation rate ($k_d \sim 0.0010$ s^{-1}), and fitting of the data correlated well with the 1:1 binding model. The longest injection series (750 s) possessed the slowest dissociation rate ($k_d \sim 0.0002$ s^{-1}), but fitting of the data did not agree with the 1:1 binding model. The middle injection series (375 s) possessed an intermediate dissociation rate ($k_d \sim 0.0004$ s^{-1}), and fitting of the data also did not agree with the 1:1 binding model. Evaluation of the contact time test results revealed poor correlations with the 1:1 model, and the decreasing dissociation rate constants (with increasing contact time) are consistent with the two-state kinetic model described in the BIAevaluation software. Thus, the initial binding of analyte and ligand would have occurred during the association phase, and a subsequent conformational change in the plasminogen-apo(a) complex may account for the altered rate constants in the dissociation phase.

Evaluation of the dose−response titrations revealed an equilibrium dissociation constant (K_D) of ~0.3 μM for Glu[1]-plasminogen binding to wild-type or citraconic anhydride-modified 17K r-apo(a). On the basis of the wild-type 17K r-apo(a) titrations, estimated rate constants for the association ($k_a \sim 1500$ M^{-1} s^{-1}) and dissociation ($k_d \sim 0.0005$ s^{-1}) phases are indicative of relatively slow binding kinetics between Glu[1]-plasminogen and apo(a) overall. In contrast, the majority of plasminogen fragments (PgK1−5, PgK1−3, PgK4, and PgK5P) exhibited low levels of rapid, steady-state binding compared to the hyperbolic isotherms seen with native Glu[1]-plasminogen (Figure 3A). For example, equilibrium binding experiments estimated a K_D of ~50 μM for the interaction between PgK1−3 and 17K r-apo(a) (Figure 4). A linear profile in the corresponding Scatchard analysis also indicated that a single class of binding sites is involved in this interaction. No significant binding was observed with the plasminogen tail domain and, interestingly, Lys[78]-plasminogen exhibited biphasic isotherms (Figure 3A). Compared to Glu[1]-plasminogen, significantly more Lys[78]-plasminogen bound to the 17K r-apo(a) surface due to the presence of an additional, rapid binding event at the start of the association phase. Moreover, significantly less Lys[78]-plasminogen remained on the 17K r-apo(a) surface due to the presence of an additional, rapid dissociation event at the start of the dissociation phase. Evaluation of the mid-sections of the association (150−600 s) and dissociation (900−1350 s) phases, however, revealed that the estimated on- and off-rates (k_a and k_d, respectively) in these regions did not differ significantly between the Glu[1]-plasminogen and Lys[78]-plasminogen injections. Thus, although the overall affinities ($K_D = k_d/k_a$) of Glu[1]- and Lys[78]-plasminogen for 17K r-apo(a) are similar, Lys[78]-plasminogen binding to apo(a) is more complicated and weaker overall due to additional interactions not apparent with Glu[1]-plasminogen binding.

Subsequent experiments in which Glu[1]-plasminogen was injected in the presence of variable chloride and acetate concentrations generated dramatically different binding profiles (Figure 3B). While ionic strength was held constant, monophasic isotherms in the presence of chloride (ie. closed Glu[1]-plasminogen conformation) shifted to biphasic isotherms in the presence of acetate. The biphasic Glu[1]-plasminogen isotherms possessed an additional, rapid binding event at the start of the association phase followed by the

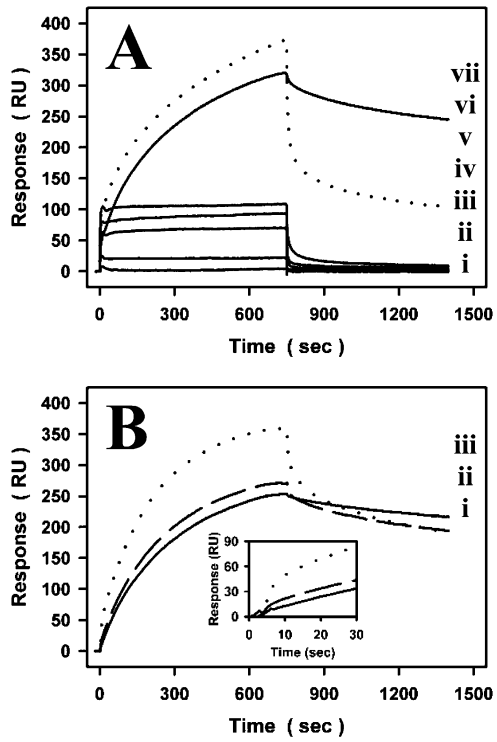

FIGURE 3: SPR analysis of plasminogen fragment analytes binding to apo(a) ligand at 20 μL/min: (A) representative sensorgrams for specific binding of (i) 10 μM plasminogen tail domain, (ii) 10 μM PgK4, (iii) 10 μM PgK1−3, (iv) 10 μM PgK5P, (v) 5 μM PgK1−5, (vi) 2 μM Lys^{78}-plasminogen (dotted line), and (vii) 2 μM Glu^{1}-plasminogen (solid line) to 2700 RU of 17K r-apo(a) in the presence of 150 mM chloride/0 mM acetate; (B) representative sensorgrams for specific binding of 1 μM Glu^{1}-plasminogen to 1700 RU of 17K r-apo(a) in the presence of (i) 150 mM chloride/0 mM acetate (solid line), (ii) 75 mM chloride/75 mM acetate (dashed line), and (iii) 0 mM chloride/150 mM acetate (dotted line); (inset) corresponding analysis in which changes within the first 30 s are highlighted.

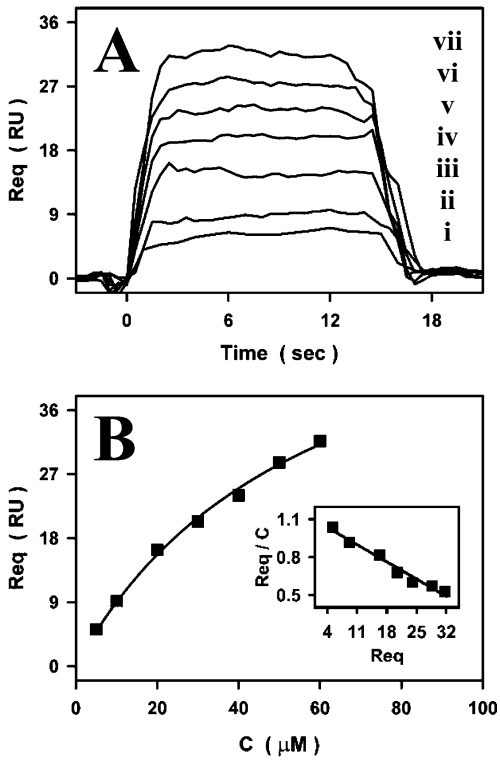

FIGURE 4: SPR analysis of PgK1−3 analyte binding to apo(a) ligand at 40 μL/min: (A) representative sensorgrams for steady-state binding of (i) 5, (ii) 10, (iii) 20, (iv) 30, (v) 40, (vi) 50, and (vii) 60 μM PgK1−3 binding to 1700 RU of 17K r-apo(a); (B) representative plot of steady-state binding in which the *symbols* correspond to experimental data and the *line* corresponds to nonlinear regression analysis of the data to an equation describing equilibrium binding; (inset) corresponding Scatchard analysis in which the *symbols* correspond to experimental data and the *line* corresponds to linear regression analysis of the data. In each panel, R_{eq} is the steady-state binding level and C is the concentration of PgK1−3 in solution.

longer, slower association event (Figure 3B inset). Increases in the Glu^{1}-plasminogen binding response and the dissociation rate were maximal in the presence of 150 mM acetate (i.e., open Glu^{1}-plasminogen conformation), yielding isotherms that were reminiscent of Lys^{78}-plasminogen in the presence of 150 mM chloride (i.e., open Lys^{78}-plasminogen conformation). Unlike Lys^{78}-plasminogen, however, the plasminogen tail domain was still intact in the chloride/acetate experiments performed with Glu^{1}-plasminogen.

Fluorescence spectroscopy analyses were then employed to investigate conformational changes in the SPR analyte/ligand in the presence of variable chloride and acetate concentrations. Glu^{1}-plasminogen and 17K r-apo(a) were titrated with ϵ-ACA in 150 mM chloride- or actetate-containing buffers identical to those utilized in the SPR experiments. The intrinsic fluorescence of Glu^{1}-plasminogen (150 nM) in chloride buffer increased ~10% when ϵ-ACA was titrated to 20 mM, whereas the identical experiment in acetate buffer resulted in an increase of only ~4% (Figure 5A,B). The intrinsic fluorescence of 17K apo(a) (70 nM) decreased ~15% in either chloride or acetate buffer when ϵ-ACA was titrated to 100 mM (Figure 5C,D). Taken together, the titrations suggest that the native conformation of 17K r-apo(a) was unaltered in the SPR experiments by the change in anions, whereas Glu^{1}-plasminogen would have adopted a more open, relaxed, "Lys^{78}-plasminogen"-like conformation in the presence of acetate (compared to its native, closed conformation in the presence of chloride).

To examine the functional consequence of the differential SPR kinetics observed between Glu^{1}-/Lys^{78}-plasminogen and apo(a), fluorescent plasminogen activation assays were performed with soluble FDP cofactors (Figure 6). Cleavage of the fluorescently labeled plasminogens by tPA elicits a conformational change that results in a quenching of the fluorescein fluorescence. Because the active site serine has been mutated to a cysteine in the recombinantly expressed plasminogen, the fluorescent Glu^{1}- and Lys^{78}-plasmin products formed remain catalytically inactive, thereby simplifying the kinetics of the reaction. The kinetic plots (relative fluorescence vs time) presented are typical of results acquired in at least three independent trials. Overall, it was found that 17K r-apo(a) inhibited the rates of Glu^{1}-plasminogen activation in a dose-dependent manner (Figure 6A) but failed to inhibit Lys^{78}-plasminogen activation under similar assay conditions (Figure 6B).

DISCUSSION

Previous fluorescence studies with a series of recombinant apo(a) variants have shown that the apo(a) protease-like domain mediates binding to Glu^{1}-plasminogen in solution (*38*). Exposed lysine residues in the apo(a) protease-like

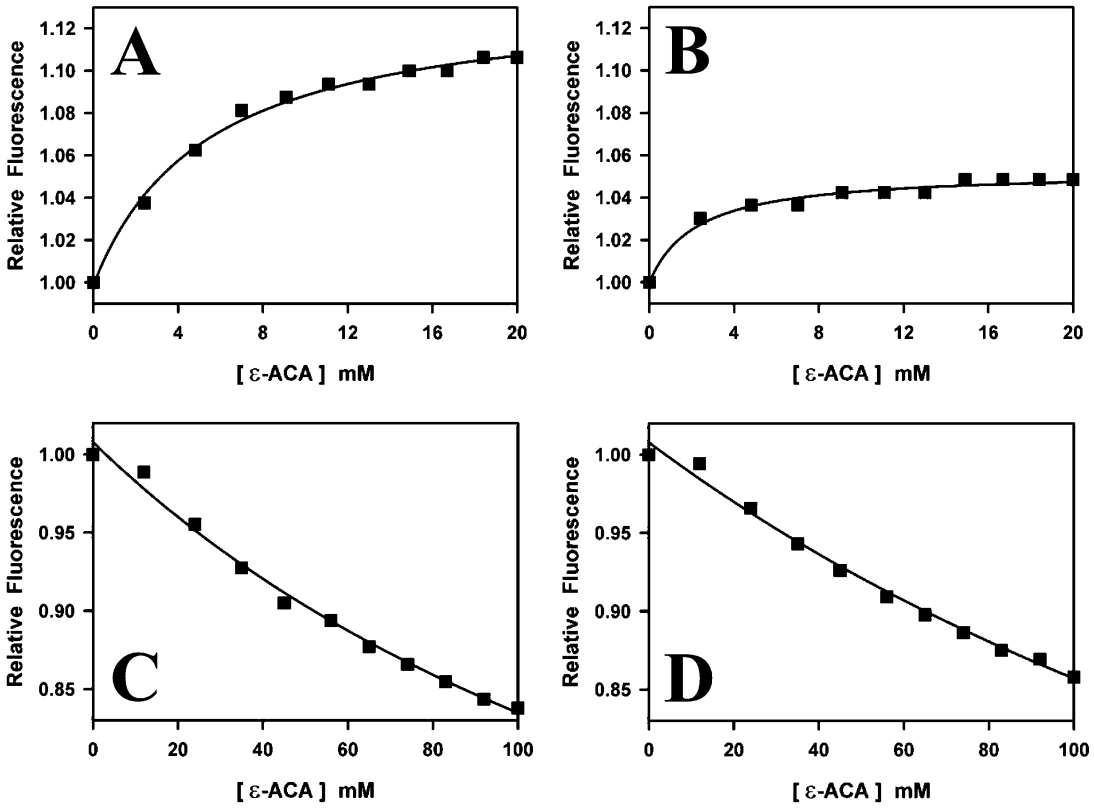

FIGURE 5: Fluorescence spectroscopy of ϵ-ACA binding to Glu^1-plasminogen and apo(a): representative intrinsic fluorescence titrations of ϵ-ACA binding to 150 nM Glu^1-plasminogen in the presence of 150 mM chloride (A), 150 nM Glu^1-plasminogen in the presence of 150 mM acetate (B), 70 nM 17K r-apo(a) in the presence of 150 mM chloride (C), and 70 nM 17K r-apo(a) in the presence of 150 mM acetate (D). In each panel, the *symbols* correspond to experimental data and the *lines* correspond to nonlinear regression analysis of the data to an equation describing equilibrium binding.

domain are hypothesized to interact with LBS in plasminogen. Conversely, the present study sought to determine which kringle domains in plasminogen are important for mediating binding to apo(a).

Methods initially chosen to examine the binding between the isolated plasminogen fragments and apo(a) (i.e., ELISA, RIA, intrinsic and extrinsic fluorescence) all proved to be problematic for a variety of reasons beyond the scope of this publication. On the other hand, SPR successfully addressed the current objective in a quantitative, real-time manner. Initial SPR experiments using amine-coupled apo(a) or plasminogen as the ligand proved to be confounding, however, due to the lysine-dependent nature of the binding interaction. This approach also generated less desirable heterogeneous surfaces for kinetic studies, and certain amine-coupled plasminogen surfaces (i.e., PgK4) were very unstable as previously reported (*51*). Capture techniques using amine-coupled apo(a)- or plasminogen-specific monoclonal antibodies also failed to yield reliable data. Eventually, the ligand thiol immobilization technique provided stable, oriented, homogeneous surfaces. The 17K r-apo(a) was thiol-coupled to the CM5 sensor chip surface through the unpaired cysteine in KIV_9, thereby mimicking how apo(a) is disulfide-bonded to apoB-100 in the intact Lp(a) particle.

Using immobilized surfaces of the appropriate density, increases in the SPR signal allowed monitoring of the smaller molecular weight plasminogen/fragment analytes (9−92 kDa) binding to the larger molecular weight apo(a) ligand (279 kDa). The interaction was also very specific as binding of Glu^1-plasminogen to 17K r-apo(a) was unaltered in the presence of BSA or high-salt conditions. Binding was altered, however, in the presence of the lysine analogue ϵ-ACA, citraconic anhydride-modified Glu^1-plasminogen, and 17K r-apo(a) as solution-phase competitors. All of these methods to decrease and/or abolish binding reinforced the lysine-dependent nature of this interaction that has been demonstrated in our previous work (*38*). The present study, however, has challenged the notion that lysine residues on apo(a) interact only with LBS in plasminogen. The SPR experiments with citraconic anhydride modification have illustrated that lysine residues on 17K r-apo(a) are indeed important, but lysine residues on Glu^1-plasminogen also appear to be critical for apo(a)-plasminogen binding to occur.

Initial dose−response titrations for native, Glu^1-plasminogen binding to 17K r-apo(a) failed to conform to a simple "1:1 binding" model using the BIAevaluation software. Because flow rate tests with low-density immobilized surfaces successfully ruled out any mass transport limitations, deviations from 1:1 binding were then thought to reflect the fact that purified plasminogen is naturally heterogeneous. In plasma, native plasminogen is composed of two glycoforms (*6*): 35% Glu^1-plasminogen I (glycosylated at Asn^{289} and Thr^{346}) and 65% Glu^1-plasminogen II [glycosylated at Thr^{346} only; plasminogen amino acid numbering system includes Gln residue at sequence position 32 (see ref *44*)]. The two glycoforms differ structurally and functionally in terms of their native conformations (*52*), affinities for lysine−Sepharose (*53*), and rates of plasminogen activation (*54*). Once the contact time test was performed, however, we found that short contact times yielded 1:1 binding, whereas longer

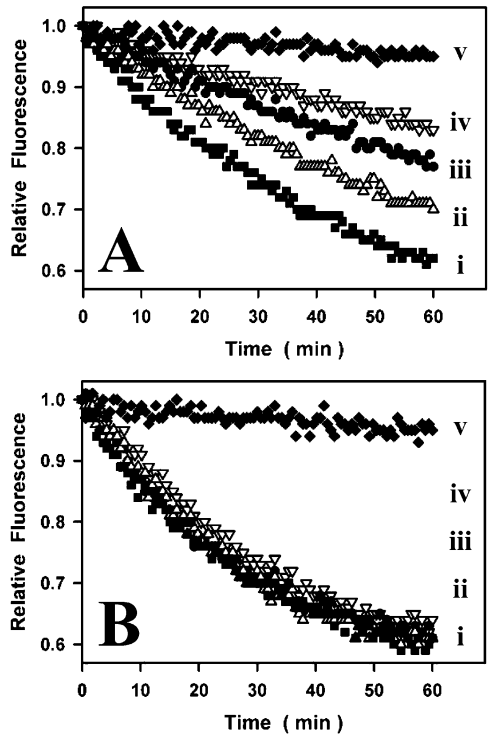

FIGURE 6: Fluorescent plasminogen activation assay to examine the inhibition of tPA-mediated plasminogen activation by apo(a): representative kinetic plots for the activation of 0.3 μM Flu-Glu^1-plasminogen (A) or 0.3 μM Flu-Lys^{78}-plasminognen (B) in the presence of (i) 0 μM 17K r-apo(a), (ii) 1 μM 17K r-apo(a), (iii) 2 μM 17K r-apo(a), (iv) 3 μM 17K r-apo(a), and (v) no tPA control. In each panel, all reactions contained 0.6 μM FDP cofactor and 3 nM tPA.

contact times did not. Good 1:1 fits obtained with the short injection series were indicative that the Glu^1-plasminogen glycoforms I and II were binding to 17K r-apo(a) in identical fashion; therefore, additional SPR analyses with the isolated glycoforms were not required. On the other hand, poor 1:1 fits were obtained with the longer injection series, and the dissociation rate constants decreased in the presence of increased contact times.

Because several possible technical concerns (e.g., mass transport limitations, analyte/ligand heterogeneity) failed to account for the observed deviations from 1:1 binding, a more complex kinetic model was investigated using the BIAevaluation software. Results from the contact time test indicate that our present SPR results are consistent with a "two-state reaction (conformation change)" model for the plasminogen-apo(a) binding interaction. According to this model, analyte (A) binds to ligand (L) and the resultant complex AL changes to AL*, an alternative form of the complex that dissociates very slowly to A + L. The conformational change can occur in only the AL complex, not in free A or L. To simplify the model, it also is assumed that the only way AL* can dissociate to release free A + L is through prior conversion to the complex AL. The relative inability of AL* to dissociate directly is consistent with the very slow dissociation rate constants observed for Glu^1-plasminogen binding to 17K r-apo(a) in the longer injection series.

Loss of the plasminogen tail domain dramatically altered the binding kinetics of various plasminogen fragments for apo(a). In general, no single kringle domain in plasminogen could account for the binding response observed with native Glu^1-plasminogen. The plasminogen tail domain was the only fragment that failed to exhibit any binding to apo(a) over baseline. After adjustment for differences in molecular weight, PgK1−5, PgK1−3, PgK4, and PgK5P all exhibited effectively similar levels of weak binding relative to Glu^1-plasminogen. Despite differences between PgK1−5, PgK1−3, PgK4, and PgK5P in terms of the number and combination of lysine-binding kringles present, binding to 17K r-apo(a) was comparable. These plasminogen fragments, however, rapidly reached steady-state binding levels in contrast to the more gradual, hyperbolic isotherms observed using Glu^1-plasminogen. Interestingly, Lys^{78}-plasminogen exhibited biphasic isotherms compared to the monophasic isotherms observed with Glu^1-plasminogen. Similar biphasic isotherms were observed when the binding of intact Glu^1-plasminogen (i.e., plasminogen tail domain present) to 17K r-apo(a) was examined in the presence of variable chloride and acetate ion concentrations. This result confirmed that the biphasic isotherms were conformation-dependent and not attributable to the loss of specific sequences contained within the plasminogen tail domain, which is absent in Lys^{78}-plasminogen. Moreover, the biphasic effects observed were not due to bulk effects because all sensorgrams presented were subtracted over reference surfaces.

One of the most striking properties of Glu^1-plasminogen is its tight, activation-resistant conformation (*18*, *19*). The binding of lysine analogues to LBS in Glu^1-plasminogen elicits a large conformational change that is characterized by a sigmoidal increase in intrinsic fluorescence with increasing analogue concentration. Previous studies have reported fluorescence intensity increases of 7.5−10% upon Glu^1-plasminogen binding to ϵ-ACA (0−16 mM) in chloride-containing buffers (*46*, *55*). In contrast, no significant increase in intrinsic fluorescence is observed upon Lys^{78}-plasminogen binding to ϵ-ACA under similar conditions (*18*). Thus, Glu^1-plasminogen is characterized by a closed conformation, whereas Lys^{78}-plasminogen is characterized by an open conformation. Upon binding to lysine analogues, apo(a) also undergoes a large conformational change that can be monitored by intrinsic fluorescence. Previous studies from our laboratory have reported a fluorescence decrease of 15−20% upon 17K r-apo(a) binding to ϵ-ACA (0−100 mM) in chloride-containing buffers (*50*). Although analogous to the conformational change in plasminogen, the molecular determinants that govern the conformational change in apo(a) are dissimilar to those that govern the conformational change in plasminogen (*50*).

It is well established that chloride ions help to maintain the closed conformation of native Glu^1-plasminogen, whereas other ions such as acetate cause Glu^1-plasminogen to adopt a more open, relaxed conformation like that of Lys^{78}-plasminogen (*15*). In agreement with the literature values noted above, intrinsic Glu^1-plasminogen titrations with ϵ-ACA in our study resulted in an overall fluorescence increase of 10% in the presence of the chloride-containing buffer. The similar experiment performed in the presence of acetate resulted in an overall fluorescence increase of only 4%. Although no fluorescence increase is expected when Lys^{78}-plasminogen is titrated with ϵ-ACA, previous studies have indicated that positive co-operative binding of at least two ligands (ϵ-ACA, *t*-AMCHA) to Glu^1-plasminogen is required to induce a fully extended conformation of the

molecule (*16*, *20*). Specifically, it is hypothesized that initial binding to the PgK5 domain induces a conformation change that facilitates the rapid binding of a second ligand to the PgK4 domain. Although substituting chloride ions for acetate ions likely establishes equilibrium between the open and closed forms of Glu[1]-plasminogen, it is important to note that a significantly larger percentage of Glu[1]-plasminogen was in the open state in acetate as assessed by the intrinsic fluorescence titrations.

To examine the functional consequence of the differential SPR kinetics observed between Glu[1]-/Lys[78]-plasminogen and apo(a), fluorescent plasminogen activation assays were performed. Although the fluorescently labeled plasminogen remains catalytically inactive upon cleavage by tPA, the resultant conformation change results in a fluorescence decrease that can be followed in real time. Previous work with this model system has validated that the inhibition of tPA-mediated Glu[1]-plasminogen activation by Lp(a) is attributable to the apo(a) moiety; the dose-dependent inhibition observed with 17K r-apo(a) is consistent whether native fibrin or degraded fibrin (FDP) cofactors are utilized (*41*). The present fluorescent plasminogen activation results (utilizing FDP) indicate that apo(a) is a strong inhibitor of Glu[1]-plasminogen activation but a poor inhibitor of Lys[78]-plasminogen activation. These results agree with previous in vitro clot lysis assays in which apo(a) attenuated the lysis of clots prepared from purified fibrinogen and initially containing Glu[1]-plasminogen, but had no effect on the lysis of similar clots in which Lys[78]-plasminogen was substituted (*34*). Although positive feedback reactions catalyzed by plasmin would have been present in the clot lysis assays, such feedback reactions were not present in the fluorescent plasminogen activation assays. Despite such differences between the two assay systems, a common outcome has been observed in which the apo(a) inhibitor behaves differently in the fibrinolytic process depending upon whether Glu[1]- or Lys[78]-plasminogen is present.

This is the first study in which apo(a) binding to plasminogen (and its fragments) has been examined in real time by SPR. Analyte binding was examined under physiological conditions (0.15 M NaCl, pH 7.4) and in the presence of the natural molar ratio of the plasminogen glycoforms. Analyte concentrations were reflective of normal circulating plasma plasminogen levels (2−3 μM), and our immobilization technique mimicked how apo(a) is naturally disulfide-bonded in the context of the native Lp(a) particle. An estimated equilibrium dissociation constant (K_D) of ~0.3 μM for Glu[1]-plasminogen binding to 17K r-apo(a) by SPR is in good agreement with previously acquired binding data using radioiodinated 17K r-apo(a) and Glu[1]-plasminogen immobilized in microtiter wells ($K_D \sim 0.2$ μM) (M. A. Hancock and M. L. Koschinsky, unpublished results). In contrast, we previously reported an equilibrium dissociation constant of ~20 nM for the solution-phase interaction between 17K r-apo(a) and fluorescently labeled plasminogen (*38*). The decreased affinity of this interaction in our present SPR studies may reflect a more restricted 17K r-apo(a) conformation when thiol-coupled to the CM5 sensor chip surface.

Overall, we have shown that all structural domains in native Glu[1]-plasminogen are important for maximal, high-affinity binding to apo(a) and that a variety of truncated plasminogen fragments exhibit decreased binding affinities. We have also shown that changes in the native conformation of plasminogen (i.e., Glu[1]- to Lys[78]-plasminogen conversion) dramatically alter its binding interaction with thiol-coupled apo(a) as well as the ability of apo(a) to inhibit plasminogen activation on a FDP surface. Whereas Glu[1]-plasminogen binding to apo(a) was characterized by a single binding interaction (monophasic isotherm), Lys[78]-plasminogen binding was characterized by more than one binding interaction (biphasic isotherm). Thus, it appears that Glu[1]- to Lys[78]-plasminogen conversion may result in the exposure of additional apo(a) binding sites. Moreover, modeling of our data indicated that Glu[1]-plasminogen binding to apo(a) is consistent with a two-state kinetic model, which suggests that a conformational change in the plasminogen-apo(a) complex is occurring. Additional biophysical studies are required to provide direct evidence that a conformational change is taking place.

All of the current results may be relevant to the mechanism underlying the ability of apo(a) to inhibit tPA-mediated Glu[1]-plasminogen activation. Our previous kinetic studies using fluorescently labeled plasminogen suggest that apo(a) participates in a quaternary apo(a)−cofactor-tPA−plasminogen complex that exhibits a lower turnover number (with respect to plasmin formation) compared to the corresponding ternary complex lacking apo(a) (*41*). The nature of the interactions between apo(a) and the other three components is unknown. One interpretation of our findings is that apo(a) interacts with multiple domains in plasminogen, because weak interactions were observed between apo(a) and all plasminogen fragments examined. As a result, apo(a) may interfere with binding interactions between plasminogen and tPA and/or cofactor (fibrin, FDP). Alternatively, the conformational change in the plasminogen−apo(a) complex predicted by the SPR model may result in a form of plasminogen that is less readily activated or is impaired in its interaction with tPA and/or cofactor. Further structural and functional analyses of both apo(a) and plasminogen will be required to address these questions.

ACKNOWLEDGMENT

We thank Dr. Jean Grundy and Dr. Ed Pryzdial (Canadian Blood Services) for their assistance with the N-terminal sequencing of the elastase-derived plasminogen fragments. We also thank Tomoko Hirama and Dr. Roger MacKenzie (National Research Council of Canada) and Jose Gutierrez and Dr. Jimmy Page (Biacore Inc.) for their contributions to the surface plasmon resonance experiments. In addition, we thank Dr. Michael E. Nesheim (Queen's University) for his contributions to the fluorescent plasminogen activation assays and fluorescence spectroscopy analyses. Finally, we thank Dr. Michael B. Boffa (Queen's University) for his critical review and comments during the preparation of the manuscript.

REFERENCES

1. Marcovina, S. M., and Koschinsky, M. L. (2003) Evaluation of lipoprotein(a) as a prothrombotic factor: progress from bench to bedside, *Curr. Opin. Lipidol. 14*, 361−366.
2. Berg, K. (1963) A new serum type system in man−the Lp system, *Acta Pathol. Microbiol. Scand. 59*, 369−382.
3. Koschinsky, M. L., Côté, G., Gabel, B., and van der Hoek, Y. Y. (1993) Identification of the cysteine residue in apolipoprotein(a) that mediates extracellular coupling with apolipoprotein B-100, *J. Biol. Chem. 268*, 19819−19825.

4. Brunner, C., Kraft, H.-G., Utermann, G., and Müller, H.-J. (1993) Cys4057 of apolipoprotein(a) is essential for lipoprotein(a) assembly, *Proc. Natl. Acad. Sci. U.S.A. 90*, 11643−11647.
5. McLean, J. W., Tomlinson, J. E., Kuang, W.-J., Eaton, D. L., Chen, E. Y., Fless, G. M., Scanu, A. M., and Lawn, R. M. (1987) cDNA sequence of human apolipoprotein(a) is homologous to plasminogen, *Nature 330*, 132−137.
6. Sottrup-Jensen, L., Claeys, H., Zajdel, M., Petersen, T. E., and Magnussen, S. (1978) The primary structure of human plasminogen: isolation of two lysine-binding fragments and one "mini"-plasminogen (MW, 38000) by elastase-catalyzed-specific limited proteolysis, in *Progress in Chemical Fibrinolysis and Thrombolysis* (Davidson, J. F, Rowan, R. M., Samama, M. M., and Denoyers, P. C., Eds.), pp 191−209, Raven Press Publishers, New York.
7. Forsgren, M., Raden, B., Israelsson, M., Larsson, K., and Heden, L.-O. (1987) Molecular cloning and characterization of a full-length cDNA clone for human plasminogen, *FEBS Lett. 213*, 254−260.
8. Hoover, G. J., Menhart, N., Martin, A., Warder, S., and Castellino, F. J. (1993) Amino acids of the recombinant kringle 1 domain of human plasminogen that stabilize its interaction with omega-amino acids, *Biochemistry 32*, 10936−10943.
9. Marti, D., Schaller, J., Ochensberger, B., and Rickli, E. E. (1994) Expression, purification, and characterization of the recombinant kringle 2 and kringle 3 domains of human plasminogen and analysis of their binding affinity for omega-aminocarboxylic acids, *Eur. J. Biochem. 219*, 455−462.
10. McCance, S. G., Menhart, N., and Castellino, F. J. (1994) Amino acid residues of the kringle-4 and kringle-5 domains of human plasminogen that stabilize their interactions with omega-amino acid ligands, *J. Biol. Chem. 269*, 32405−32410.
11. An, S. S. A., Carreno, C., Marti, D. N., Schaller, J., Albericio, F., and Llinas, M. (1998) Lysine-50 is a likely site for anchoring the plasminogen N-terminal peptide to lysine-binding kringles, *Protein Sci. 7*, 1960−1969.
12. Cockell, C. S., Marshall, J. M., Dawson, K. M., Cederholm-Williams, S. A., and Ponting, C. P. (1998) Evidence that the conformation of unliganded human plasminogen is maintained via an intramolecular interaction between the lysine-binding site of kringle 5 and the N-terminal peptide, *Biochem. J. 333*, 99−105.
13. Lucas, M. A., Fretto, L. J., and McKee, P. A. (1983) The binding of human plasminogen to fibrin and fibrinogen, *J. Biol. Chem. 258*, 4249−4256.
14. Chibber, B. A. K., and Castellino, F. J. (1986) Regulation of streptokinase-mediated activation of human plasminogen by fibrinogen and chloride ions, *J. Biol. Chem. 261*, 5289−5295.
15. Urano, T., Chibber, B. A. K., and Castellino, F. J. (1987) The reciprocal effects of epsilon-aminohexanoic acid and chloride ion on the activation of human [Glu1] plasminogen by human urokinase, *Proc. Natl. Acad. Sci. U.S.A. 84*, 4031−4034.
16. Marshall, J. M., Brown, A. J., and Ponting, C. P. (1994) Conformational studies of human plasminogen and plasminogen fragments: evidence for a novel third conformation of plasminogen, *Biochemistry 33*, 3599−3606.
17. Markus, G., Evers, J. L., and Hobika, G. H. (1978) Comparison of some properties of native (Glu) and modified (Lys) human plasminogen, *J. Biol. Chem. 253*, 733−739.
18. Violand, B. N., Byrne, R., and Castellino, F. J. (1978) The effect of alpha-, omega-amino acids on human plasminogen structure and activation, *J. Biol. Chem. 253*, 5395−5401.
19. Mangel, W. F., Lin, B. H., and Ramakrishnan, V. (1990) Characterization of an extremely large, ligand-induced conformational change in plasminogen, *Science 248*, 69−73.
20. Christensen, U., and Molgaard, L. (1992) Positive co-operative binding at two weak lysine-binding sites governs the Glu-plasminogen conformational change, *Biochem. J. 285*, 419−425.
21. Ramakrishnan, V., Patthy, L., and Mangel, W. F. (1991) Conformation of Lys-plasminogen and the kringle 1−3 fragment of plasminogen analysed by small-angle neutron scattering, *Biochemistry 30*, 3963−3969.
22. Hoylaerts, M., Rijken, D. C., Lijnen, H. R., and Collen, D. (1982) Kinetics of the activation of plasminogen by human tissue plasminogen activator: role of fibrin, *J. Biol. Chem. 257*, 2912−2919.
23. Fredenburgh, J. C., and Nesheim, M. E. (1992) Lys-plasminogen is a significant intermediate in the activation of Glu-plasminogen during fibrinolysis in vitro, *J. Biol. Chem. 267*, 26150−26156.
24. Lackner, C., Cohen, J. C., and Hobbs, H. H. (1993) Molecular definition of the extreme size polymorphism in apolipoprotein-(a), *Hum. Mol. Genet. 2*, 933−940.
25. van der Hoek, Y. Y., Wittekoek, M. E., Beisiegel, U., Kastelein, J. J. P., and Koschinsky, M. L. (1993) The apolipoprotein(a) kringle IV repeats which differ from the major repeat kringle are present in variably-sized isoforms, *Hum. Mol. Genet. 2*, 361−366.
26. Marcovina, S. M., Hobbs, H. H., and Albers, J. J. (1996) Relation between number of apolipoprotein(a) kringle IV repeats and mobility of isoforms in agarose gel: basis for a standardized isoform nomenclature, *Clin. Chem. 42*, 436−439.
27. Ernst, A., Helmhold, M., Brunner, C., Petho-Schramm, A., Armstrong, V. W., and Müller, H.-J. (1995) Identification of two functionally distinct lysine-binding sites in kringle 37 and in kringles 32−36 of human apolipoprotein(a), *J. Biol. Chem. 270*, 6227−6234.
28. Gabel, B. R., May, L. F., Marcovina, S. M., and Koschinsky, M. L. (1996) Lipoprotein(a) assembly: quantitative assessment of the role of apo(a) kringle IV types 2−10 in particle formation, *Arterioscler. Thromb. Vasc. Biol. 16*, 1559−1567.
29. Gabel, B. R., and Koschinsky, M. L. (1998) Sequences within apolipoprotein(a) kringle IV types 6−8 bind directly to low-density lipoprotein and mediate noncovalent association of apolipoprotein-(a) with apolipoprotein B-100, *Biochemistry 37*, 7892−7898.
30. Harpel, P. C., Gordon, B. R., and Parker, T. S. (1989) Plasmin catalyses binding of lipoprotein(a) to immobilized fibrinogen and fibrin, *Proc. Natl. Acad. Sci. U.S.A. 86*, 3847−3851.
31. Sangrar, W., Marcovina, S. M., and Koschinsky, M. L. (1994) Expression and characterization of apolipoprotein(a) kringle IV types 1, 2, and 10 in mammalian cells, *Protein Eng. 7*, 723−731.
32. Gabel, B. R., and Koschinsky, M. L. (1995) Analysis of the proteolytic activity of a recombinant form of apolipoprotein(a), *Biochemistry 34*, 15777−15784.
33. Palabrica, T. M., Liu, A. C., Aronovitz, M. J., Furie, B., Lawn, R. M., and Furie, B. C. (1995) Antifibrinolytic activity of apolipoprotein(a) in vivo: human apolipoprotein(a) transgenic mice are resistant to tissue plasminogen activator-mediated thrombolysis, *Nat. Med. 1*, 256−259.
34. Sangrar, W., Bajzar, L., Nesheim, M. E., and Koschinsky, M. L. (1995) Antifibrinolytic effect of recombinant apolipoprotein(a) in vitro is primarily due to attenuation of tPA-mediated Glu-plasminogen activation, *Biochemistry 34*, 5151−5157.
35. Biemond, B. J., Friederich, P. W., Koschinsky, M. L., Levi, M., Sangrar, W., Xia, J., Buller, H. R., and ten Cate, J. W. (1997) Apolipoprotein(a) attenuates endogenous fibrinolysis in the rabbit jugular vein thrombosis model in vivo, *Circulation 96*, 1612−1615.
36. Loscalzo, J., Weinfeld, M., Fless, G. M., and Scanu, A. M. (1990) Lipoprotein(a), fibrin binding, and plasminogen activation, *Arteriosclerosis 10*, 240−245.
37. Klezovitch, O., Edelstein, C., and Scanu, A. M. (1996) Evidence that the fibrinogen binding domain of apo(a) is outside the lysine binding site of kringle IV-10: a study involving naturally occurring lysine binding defective lipoprotein(a) phenotypes, *J. Clin. Invest. 98*, 185−191.
38. Sangrar, W., Gabel, B. R., Boffa, M. B., Walker, J. B., Hancock, M. A., Marcovina, S. M., Horrevoets, A. J. G., Nesheim, M. E., and Koschinsky, M. L. (1997) The solution phase interaction between apolipoprotein(a) and plasminogen inhibits the binding of plasminogen to a plasmin-modified fibrinogen surface, *Biochemistry 36*, 10353−10363.
39. Sangrar, W., and Koschinsky, M. L. (2000) Characterization of the interaction of recombinant apolipoprotein(a) with modified fibrinogen surfaces and fibrin clots, *Biochem. Cell Biol. 78*, 519−525.
40. Simon, D. I., Fless, G. M., Scanu, A. M., and Loscalzo, J. (1991) Tissue-type plasminogen activator binds to and is inhibited by surface-bound lipoprotein(a) and low-density lipoprotein, *Biochemistry 30*, 6671−6677.
41. Hancock, M. A., Boffa, M. B., Marcovina, S. M., Nesheim, M. E., and Koschinsky, M. L. (2003) Inhibition of plasminogen activation by lipoprotein(a): critical domains in apolipoprotein-(a) and mechanism of inhibition on fibrin and degraded fibrin surfaces, *J. Biol. Chem. 278*, 23260−23269.
42. Bajzar, L., Manuel, R., and Nesheim, M. E. (1995) Purification and characterization of TAFI, a thrombin-activable fibrinolysis inhibitor, *J. Biol. Chem. 270*, 14477−14484.

43. Koschinsky, M. L., Tomlinson, J. E., Zioncheck, T. F., Schwartz, K., Eaton, D. L., and Lawn, R. M. (1991) Apolipoprotein(a): expression and characterization of a recombinant form of the protein in mammalian cells, *Biochemistry 30*, 5044−5051.
44. Castellino, F. J., and Powell, J. R. (1981) Human plasminogen, *Methods Enzymol. 80*, 365−378.
45. Becker, L., McLeod, R. S., Marcovina, S. M., Yao, Z., and Koschinsky, M. L. (2001) Identification of a critical lysine residue in apolipoprotein B-100 that mediates noncovalent interaction with apolipoprotein(a), *J. Biol. Chem. 276*, 36155−36162.
46. Horrevoets, A. J. G., Pannekoek, H., and Nesheim, M. E. (1997) Production and characterization of recombinant human plasminogen-(S741C-fluorescein): a novel approach to study zymogen activation without generation of active protease, *J. Biol. Chem. 272*, 2176−2182.
47. Keesler, G. A., Li, Y., Skiba, P. J., Fless, G. M., and Tabas, I. (1994) Macrophage foam cell lipoprotein(a)/apolipoprotein(a) receptor: cell-surface localization, dependence of induction on new protein synthesis, and ligand specificity, *Arterioscler. Thromb. 14*, 1337−1345.
48. Wu, H. L., Chang, B. I., Wu, D. H., Chang, L. C., Gong, C. C., Lou, K. L., and Shi, G. Y. (1990) Interaction of plasminogen and fibrin in plasminogen activation, *J. Biol. Chem. 265*, 19658−19664.
49. Jonsson, U., Fagerstam, L., Ivarsson, B., Johnsson, B., Karlsson, R., Lundh, K., Lofas, S., Persson, B., Roos, H., Ronnberg, I., Sjolander, S., Svenberg, E., Stahlberg, R., Urbaniczky, C., Ostlin, H., and Malmqvist, M. (1991) Real-time biospecific interaction analysis using surface plasmon resonance and a sensor chip technology, *Bio Techniques 11*, 620−627.
50. Becker, L., Webb, B. A., Chitayat, S., Nesheim, M. E., and Koschinsky, M. L. (2003) A ligand-induced conformational change in apolipoprotein(a) enhances covalent Lp(a) formation, *J. Biol. Chem. 278*, 14074−14081.
51. Goretzki, L., Lombardo, C. R., and Stallcup, W. B. (2000) Binding of the NG2 proteoglycan to kringle domains mediates the functional properties of angiostatin and plasmin(ogen), *J. Biol. Chem. 275*, 28625−28633.
52. Molgaard, L., Ponting, C. P., and Christensen, U. (1997) Glycosylation at Asn-289 facilitates the ligand-induced conformational changes of human Glu-plasminogen, *FEBS Lett. 405*, 363−368.
53. Traas, D. W., Hoegee-de Nobel, B., and Nieuwenhuizen, W. (1984) Factors influencing the separation of glu-plasminogen affinity forms I and II by affinity chromatography, *Thromb. Haemostas. 52*, 347−349.
54. Takada, A., and Takada, Y. (1983) The activation of two isozymes of glu-plasminogen (I and II) by urokinase and streptokinase, *Thromb. Res. 30*, 633−642.
55. Horrevoets, A. J. G., Smilde, A. E., Fredenburgh, J. C., Pannekoek, H., and Nesheim, M. E. (1995) The activation-resistant conformation of recombinant human plasminogen is stabilized by basic residues in the amino-terminal hinge region, *J. Biol. Chem. 270*, 15770−15776.

BI048756O